



Counter-Rotating Hoop Stabilizer and SVR Control for Two-Wheels Vehicle Applications

A.Karthikeya¹, B.Shivam², M.Naveen³, K.Manjunath Reddy⁴

Dr. T. Rajesh, Ph.D⁵

^{1,2,3,4}(Department of Electrical And Electronic Engineering),⁵(Associate Professor - Department of Electrical And Electronics Engineering)

^{1,2,3,4,5}(J.B. Institute of Engineering and Technology, Hyderabad – 500075)

Corresponding Author: A.Karthikeya

ABSTRACT: The question of adjustment has consistently stood out from both scholarly world and industry. Simple stabilizer designs have been considered for kickboards, scooters, and bikes, but they are rarely used in commercial products. In this exploration, a limited scale, adjustable, two-wheels configuration, is proposed what's more, associated with a retroactive shut circle control unit for the programmed rectification of the destabilization during the movement. The plan depends on two counter- turning wheels, turned into movement toward the start of the ride and constrained by an **Inertial Estimation Unit (IMU)** sensor. The two DC engines controlling the turning of the adjusting wheels are changed through Heartbeat Width Balance (PWM) contribution to the 0 ~ 255 PWM range. An **ARDUINO** Uno Rev3 microcontroller and a **Support Vector Regression (SVR)** model with a **Radial Basis Function (RBF)** kernel comprise the control. On the off chance that a precise deviation outside the client characterized range is identified by the **IMU** sensor, the prepared SVR-RBF model predicts the expected **PWM** worth to restore harmony and conveys the messages to one or both DC engines. The proposed design was prepared and approved in a $\pm 21^\circ$ range, bringing about a 100 percent rectification exactness up to a $\pm 23^\circ$ range, though, for more noteworthy points up to

$\pm 30^\circ$, a drop in exhibitions was noticed. What's more, when a arbitrary speed increase in the $\pm 6^\circ/s^2$ range was applied, the proposed plan showed an exceptional capacity of anticipating the right **PWM** values, for both response wheels, equipped for restoring harmony in the framework inside a normal intercession time equivalent to 1.28s.

INDEX TERMS IMU, SVR, RBF

Received 26 Feb., 2024; Revised 28 Feb., 2024; Accepted 12 Mar., 2024 © The author(s) 2024.

Published with open access at www.questjournals.org

I. INTRODUCTION

Response Wheel Pendulum (RWP) is an adjustment gadget, created by Spong et al. [1], comprising of a pole associated to a pivoted support on one side and a turning wheel on the opposite side. The RWP is a reexamined variant of the transformed pendulum, in view of a neighborhood criticism linearization of the nonlinear unique framework. Beginning from an inclined position, the reaction during the swing-up stage and exactness in the partner supervisor organizing the audit of this original copy and supporting it for distribution was Mauro Tucci. Accomplishing upstanding balance have been explored by considering straight [2], [3], [4], non-direct [1], [3], [5], furthermore, more as of late the Lyapunov hypothesis [6], [7] control approaches. Straight controls might be a possibility for basic or on the other hand sluggish responding frameworks [7] while additional strong methodologies, for example, the Sliding Mode Control (SMC), Vital SMC (ISMC), and Terminal SMC (TSMC), are equipped for following what's more, controlling the direction with high exactness and low response time [8], [9], [10]. In advanced mechanics, Wheeled Adjusted Frameworks (WBS) of various calculations have been utilized, combined with shut loop controls and criticism linearization, for direction control [11] furthermore, adjustment [12]. One of the principal utilizations of WBS is addressed by two-wheels frameworks, for example, automated stages, where the stabilizer wheel is introduced away from what's more, symmetrical to the movement wheel pivot [13]. In such applications, force balance for the instance of little rakish

deviations is accomplished all the more actually and considers energy saving, when it is applied to the stabilizer wheel as opposed to the stage wheels. Alternately, a reaction wheel installed parallel and vertically offset to the motion wheel axis and controlled by a dynamical balancing algorithm has been added to two-wheeled robots with manipulation capabilities (Two-Wheeled Mobile Manipulator, TWMM) [14]. In both two wheeled robot frameworks [13], [14], the response wheel is used to control the place of the Focal point of Gravity (Gear-tooth) what's more, is enacted just when a deficiency of equilibrium is identified. Comparable single response wheel frameworks have been additionally applied to a two-wheeled upset pendulum able to do consequently arriving at an upstanding position [15] and to a solitary wheel robot constrained by a straight Corresponding Necessary Differential (PID) unit [16]. As a result, small-wheeled inverted pendulums are typically used by robots to explore areas with uneven surfaces or perform tasks in narrow spaces where humans cannot work [13, 14], [15], and 16]. The Fuzzy Sliding Mode Control (FSMC) and a flywheel-based gyroscopic balancer have been used to control the saddle position on bicycles, allowing for balancing of up to 7 in various disturbance scenarios [17]. Also, response wheel-based frameworks have likewise been utilized in satellite and space apparatus applications [18], [19], [20], [21]. The PID, which is based on the definition of gain values using dynamic equations [7, 16], [17], and can also correct potential under and overshooting scenarios [22], has largely been utilized in closed-loop controls due to its relative simplicity. A wheel-balanced inverted pendulum with a Linear Quadratic Regulator (LQR) controller has recently been used to stabilize it up to a 26.1 initial angular offset [23]. In any case, the adjustment is based on a predefined clockwise or counterclockwise rakish balance, which makes the 26.1° rectification length to be a matter of rakish force age by the turning wheel. A 2nd order sliding mode control verified by an Open Dynamic Engine (ODE) simulation [25], a synthetic state feedback controller with parameters optimization based on the BAT algorithm optimized through the integral of a time-weighted absolute error objective function [26], and additional contributions aimed at position tracking and system stabilization of a single reaction wheel pendulum utilized the 4th order discontinuous integral algorithm coupled with a homogeneous Lyapunov function to tune the PID gains [24]. While there are a variety of contributions to single reaction wheel systems, the RWP-based contributions to two-wheel systems are few and relatively recent. Trentin and colleagues [27], [28], and at the ends of a pendulum (bar), two reaction wheels of varying masses and sizes are connected and turned in opposite directions at different speeds. Despite the fact that the mechanism and control were set up using consolidated PID technology, there were issues with the voltage supply to the DC motors that controlled the reaction wheels. Additionally, the planned framework requires significant space, making it confounded to introduce in generally little vehicles, like bikes, kickboards, or bikes. Essentially, Baimukashev et al. [29] characterized a double pivot consistent reversed pendulum, made out of 2 wheels, what's more, thought about two control methodologies, Profound Brain Network (DNN) and Nonlinear Model Prescient Control (NMPC). The fact that ML-based approaches like the DNN outperform the reaction time of an already advanced control system like the NMPC by a factor close to seven is interesting. As summed up until this point, a large part of the work accessible in the writing concerns one-WBS and depends on PID regulators, which showed insecurity and under and overshooting risk on the off chance that the ideal addition isn't set. Additionally, single-wheel frameworks are additionally hard to control as far as bidirectional soundness since the position should cross a rakish speed equivalent to zero each time the turn bearing changes. Also, stable, and more solid frameworks depend on huge response wheels, making it challenging to apply them on standard-size two-wheels vehicles. A well- trained ML algorithm is ideal for general-purpose applications because it can be trained according to the considered loading scenario and mechanism, making it a potential solution to the various limitations of PID control units, as highlighted in [29]. To resolve every one of the issues introduced up to this point, the exploration introduced in this paper subtleties a Counter-Pivoting Band Stabilizer (CRHS) plan with a Help Vector Relapse (SVR) regulator. The two-wheel design of the proposed mechanism is mechanically decoupled and controlled by two independent DC motors. It is mounted on the same rotation axis. Toward the start of the movement, the two wheels are placed into revolution at a similar speed and in inverse bearing, adjusting each other's precise energy. When a destabilization of the framework is recognized, the rotational speed of one of the two wheels is decreased while the other one is kept steady to make a counter-speed increase and restabilize the framework near the first setpoint. The retroactive system is based on a closed-loop connection between an ARDUINO microcontroller controlled by SVR and an Inertial Measurement Unit (IMU) sensor. The Help Vector Relapse is an AI model, which can be combined with a client characterized part capability, taking into account high customization of the goal capability and the application to exceptionally nonlinear datasets In this examination, three portions have been applied to the SVR, specifically the Direct, Polynomial, and Spiral Premise Capability (RBF) part works. For the preparation of the SVR AI model, lab probes a specially fabricated CRHS framework have been completed inside the $\pm 21^\circ$ lean point range. The initial destabilization in terms of lean angle boundary conditions and the subsequent Pulse Width Modulation (PWM) input to the two DC motors that allowed for the stabilization of the CRHS system comprise the database. The Linear kernel had the shortest average reaction time, at 1.886s. In any case, because of the nonlinearity of the lean point PWM relationship, it likewise brings about the forecast of a non-zero PWM remedy for a lean point equivalent to nothing. Then again,

the SVR-RBF model showed a somewhat higher greatest response time, equivalent to 2.13s, yet in addition a adjustment exactness equivalent to 100 percent in the $\pm 21^\circ$ lean point scope of the preparation dataset. In addition, the SVR- RBF model demonstrated the capability of 100% correction accuracy up to a lean angle of 23 degrees, which is slightly outside

the training range and occurs when the initial acceleration is not zero. The utilization of arbitrary speed increase signs to the CRHS framework, and the significant amendment exactness, demonstrated the ability of the proposed CRHS framework to effectively recuperate conceivable framework destabilization, both under static and dynamic circumstances. The model created for this examination utilized a 13861 RPM DC engine, with 3D printed 150 mm width wheels made of ABS polymer. However, a scaled-up or scaled-down version of the DC motor and wheels as well as the same control unit can be used to meet the project's requirements and achieve the desired correction. The remainder of this paper is coordinated as follows. To start with, are all subtleties the mechanical plan and both equipment and programming controls. Then again, segment III contains the alignment of the SVM model in light of the characterized preparing FIGURE 2. Design for the Counter-Rotating Hoop Stabilizer. dataset, the proposed two-wheel stabilized application within the design range, and the results outside the training dataset range.

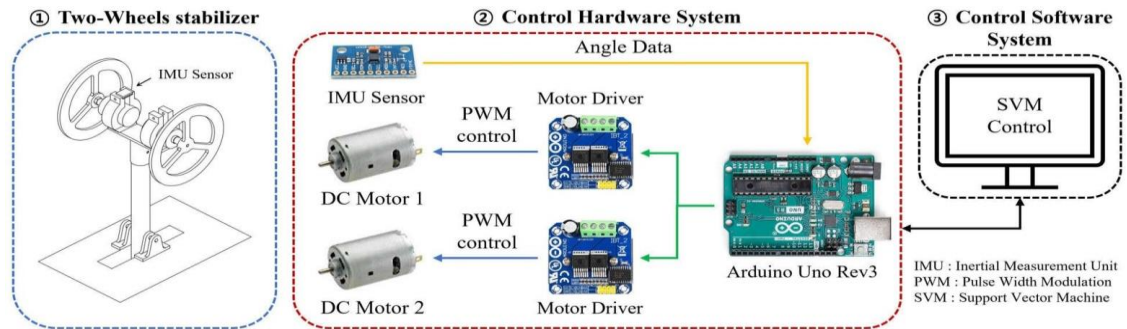


Figure 1: Conceptual representation of the three main sub-systems of the Counter-Rotating Hoop Stabilizer (CRHS).

①Mechanical two-wheels stabilizer (schematic), ② hardware system and Pulse Width Modulation (PWM) motors controls, and ③ software control based on the Support Vector Machine (SVM) machine learning model.

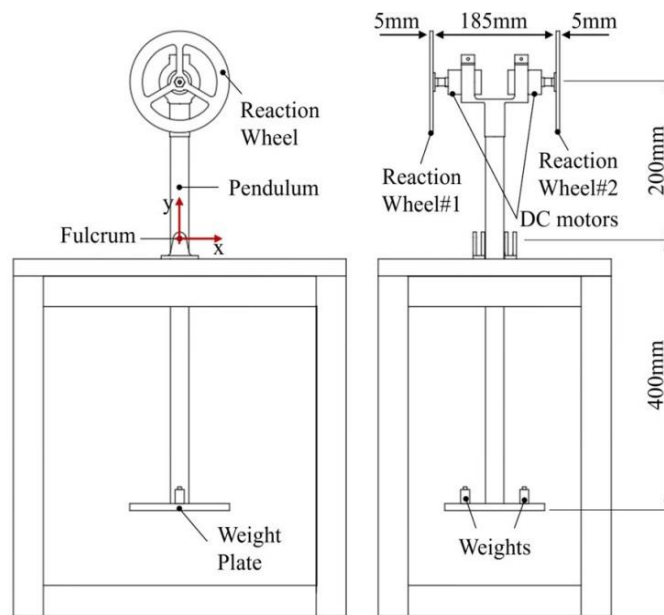


Figure 2: Counter-Rotating Hoop Stabilizer Design.

II. MATERIALS & METHODS

As depicted in Fig. 1, the Counter-Turning Loop Stabilizer (CRHS) framework is made out of three sub-frameworks. The mechanical part is addressed by the two-wheels stabilizer pendulum, the equipment (HW) unit, and the product (SW) control. The ARDUINO microcontroller and the acceleration/angle measuring sensor serve as the foundation for the hardware component, while the SVR machine learning model serves as the foundation for the software (SW) control. In order to interpret the system's dynamic response, design the appropriate correction to stabilize it, and, if necessary, correct possible under and overshooting of the target stable conditions, all three subsystems are connected in a closed loop.

A. TWO-WHEELS STABILIZER

Figure sums up the two-wheel stabilizer system that this study proposes. 2. The 150 mm-diameter thermoplastic ABS polymer wheels are connected to two 12V DC motors (HC683G-001 model, Johnson Motor Group, USA), each of which is independently controlled by two Pulse Width Modulation (PWM) modules and is controlled by an ARDUINO control unit. The pendulum is acknowledged with an empty aluminum tube associated with the support by a metallic pin, considering practically frictionless turn. The proportion between the two arms of the framework has been set to 2:1, with the more limited area associated with the principal response wheels hub and the more extended one to a weight plate. During the initial ramp-up phase, two 50 g counterweights have been added to the weight plate to stabilize all structures. Although these weights aren't heavy enough to self-stabilize in dynamic conditions, they can be used to simulate the user's control over relatively small angle ranges and static conditions. At the point when the two wheels are kicked off at something very similar rotational speed however in inverse bearings, and the pendulum has a 0° point as for the y-hub (Fig. 2), precise energy balance is laid out. In any case, if a $\neq 0$ point is presented in the framework, concerning starting limit conditions or because of the use of an outside acceleration, the rotational speed of the two wheels can be used to make a counter-speed increase to restore balance. In this exploration, the word harmony is used as far as adjustment of the precise swaying of the pendulum inside a $\pm 5^\circ$ point regarding the y-pivot.

B. CONTROL HARDWARE SYSTEM

As displayed in Fig. 1. The control HW system is a closed-loop system that uses the information from the IMU sensor (MPU- 9250, InvenSense, CA, USA) to independently control the rotational speeds of the two wheels. The in general HW framework is displayed in Fig. 3. The ARDUINO microcontroller is associated with the engine drivers controlling the two 12V DC engines, permitting the control of both rotational velocities and bearings of the two wheels. Speed is controlled regarding PWM and, for each set of PWM#1 and PWM#2, one for each engine, a brief variety of the precise second harmony can be accomplished. Since the DC motors are identical, the system is self-balanced if the IMU sensor detects no change in the pendulum angle and PWM#1 equals PWM#2. However, if a change in the pendulum angle is detected outside of a user-defined range, the signal is sent to the ARDUINO control, and a relevant change in both PWM#1 and PWM#2 is made to restore balance and stabilize the angle. For clearness, in this exploration, the control for the DC engine is communicated with regards to PWM, which compares to voltage input. The SVR model, which can be found in section II-C, was used to make a connection between the angular correction made to the system and the PWM settings for both motors. To prepare the SVR calculation, addressing the control program for the ARDUINO microcontroller, tests have been done considering an underlying rakish limit condition remembered for the $\pm 21^\circ$, furthermore, beginning speed and speed increase equivalent to nothing. Likewise, the contribution of PWM, for each engine, considering the adjustment of the framework in the $\pm 21^\circ$ range, with a 3° goal, has been procured and used as the preparing dataset for the SVR calculation.

C. CONTROL SOFTWARE SYSTEM

The AI (ML) calculation used in this research depends on the Help Vector Machine (SVM) class of calculations. Support Vector Classification (SVC) for classification problems and Support Vector Regression (SVR) for regression analyses are the two main subfields of SVM [30]. The SVC strategy recognizes the ideal parallel order choice plane in the characterized vector space. By getting a hyperplane that expands the edge, the dataset $\{(x_1, y_1), \dots, (x_n, y_n)\}$ (When x_i is X and y_i is $(-1, 1)$, the expression x_n, y_n) is used, which divides into two classes. SVC is used to order both direct and nonlinear datasets, while the last option requires the choice of a bit capability. For the instance of the SVR model, a misfortune capability is added to foresee the result factors y_n from the info factors x_n . The misfortune capability mirrors the blunder between the normal esteem and the genuine worth, and a delegate misfortune capability is ϵ -support SVR (ϵ -SVR). $\{(x_1, y_1), \dots, (x_n, y_n)\}$ (with $i = 1$ for x_n, y_n) $n(x_i, y_i) \times R$ (1) The goal of this study's - SVR is to find a regression function $f(x)$ that can interpolate the data points of (1) with a maximum error in the $[-,]$ range and the highest possible flatness of the function. (2) is the outcome of a linear regression function, where w is the variable vector. By minimizing the norm solution, the condition that a small w intrinsically leads to a high $f(x)$ flatness can be granted can be fulfilled. $f(x) = \langle w, x \rangle + b$

$\{w \in X, b \in R\}$ (2) $\|w\|_2 = \langle w, w \rangle$ (3) By taking into account through and through Eq. (Eq. is obtained by reformulating 1)-3) in terms of a convex optimization strategy. 4) where ϵ_i and $\epsilon * I$ are characterized as slack factors. The hyperparameter $C > 0$ characterizes the split the difference between evenness and permitted deviations past the $[-\epsilon, \epsilon]$ mistake range. minimize: $\frac{1}{2} \|w\|_2 + C \sum_{i=1}^n \xi_i$

D. TRAINING EXPERIMENTS

In this examination, the SVR model depicted in the past segment has been prepared by trial information connecting the PWM inputs with how much revision point applied to the pendulum. During the training, the PWM values that allowed for the reestablishment of equilibrium were categorized as positive, while those that caused undershooting or overshooting were categorized as negative. Likewise, the hyperplane and the two limit lines make three districts, as in Fig. 4. In Fig. 4, the focal green locale addresses the PWM values taking into account the adjustment of the framework in view of an underlying offset point, which could likewise be the consequence of a abrupt speed increase, brought about by off-base directing. Overshooting values (indicated in red) and undershooting values (indicated in yellow) are depicted in the areas above and below the two black dashed lines.

Focusing solely on the experimental point indicated by the "+" sign (Fig. 4), as shown in Equation (), a point in the SVR training database is represented by the combination of offset angle and PWM control. 1) [34]. The need for a consistent correlation between the lean angle and the relevant PWM signal applied to the DC motors prompted the decision to use an initial offset angle rather than an acceleration for the training dataset. Despite the fact that speed increase can be applied reliably, its estimation is more perplexing than that of an underlying offset (lean) point in this way it could prompt a problematic meaning of the preparation dataset what's more, a resulting loss of forecast exactness. On the other hand, during the field execution evaluation, introduced in segment III, both starting offset point and introductory speed increase limit conditions have been considered to reproduce genuine potential situations.

The SVR model's training and validation databases are built on the basis of a series of experiments that were conducted with the pendulum of Fig. in mind. 2, where the initial offset angle increases by a constant 3° from 6° to 21° . In each trial, the pendulum begins from a static position, enters a powerful stage when the set-point pin (Fig. 3) is taken out, and if the right PWM signal is sent to the two DC motors, it goes back to a static state. For each tried point, the PWM values has been expanded until the base adjustment input was accomplished what's more, continued expanding until overshooting happened. The summary of the dataset utilized for the training and validation of the SVR model is presented in Table 1, and the average values and standard deviations for the PWM are pertinent to the green region of Fig. 4.

Both least (6°) also, most extreme (21°) points have been characterized by fundamental tests on the proposed CRHS framework considering the trait of the PWM controls. The PWM changes the voltage of the DC engine by changing over a computerized input in the $0 \sim 255$ territory to TABLE 1. PWM adjustments values from field tests. a voltage at the end. PWM = 0 addresses 0V information though PWM = 255 is the greatest voltage input for the DC engine. The lean angle that brings the PWM signal close to its maximum of 255 is represented by 21 when taking into account the weight of the entire pendulum, as shown in Table 1. For a somewhat little lean point in the $\pm 3^\circ$ range, concerning the yaxis (Fig. 2), no destabilization was noticed, hence the lower bound has been set to 6° , as indicated by the separating of 3° . Overall, the control system is a closed loop in which the IMU sensor measures the pendulum system's angular position in real time and sends it to the ARDUINO controller for conversion into a digital (A/D) signal that is used as input by the trained SVR model. The trained SVR model sends an input to the PWM control in the event that the CRHS system becomes unstable. This causes the rotational speeds and, if necessary, directions of the two DC motors to change. This last step shuts the control circle and takes into account constant control and alignment of the CRHS framework, as displayed in Fig. 5. Within this framework, the interface between the motor control unit and the SVR algorithm, which is implemented in a laptop with a USB connection, is made possible by the ARDUINO microcontroller.

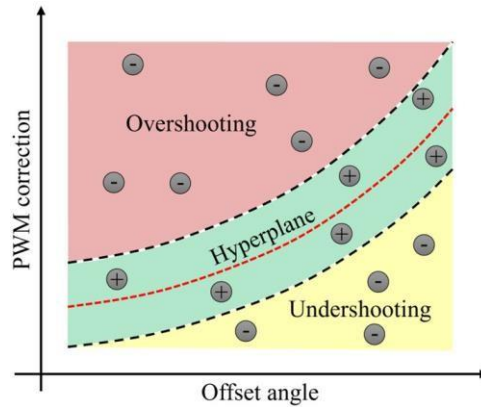


Figure 3: SVR conceptual representation of positive and negative datapoints utilized in the training and validation.

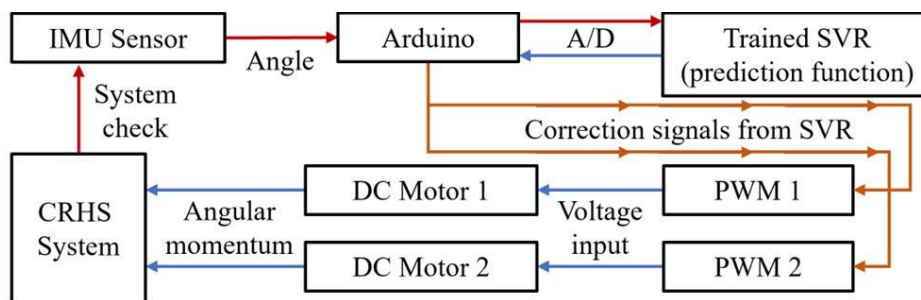


Figure 4: Signals and loop control in the CRHS system.

III. RESULTS & DISCUSSION

The outcomes introduced in this segment are coordinated by following a similar stream utilized during the turn of events of the control programming (SW) framework for the proposed Counter-Pivoting Band Stabilizer (CRHS). The relevant hyperparameters have been optimized (III-A) in order to evaluate the performance of the three kernels associated with the Support Vector Regression (SVR) model, and then their prediction capabilities have been compared to one another (III-B). Then, the entire CRHS system's field performances (Fig. 1) have been surveyed both inside the preparation precise reach also, beyond it by applying both precise and speed increase limit conditions.

A. HYPERPARAMETERS OPTIMIZATION

To compare how accurately the kernels of Eqs can predict the Pulse Width Modulation (PWM) value(9), (10), and (11), the initial step is the improvement of the hyperparameters. Through the grid search CV [35] algorithm, the search for the ideal hyperparameters begins with a random value assignment and continues until the differences between the actual and predicted PWM values are minimized. To stay away from hyperparameters overfitting, the streamlining depended on 80% of the entire exploratory data set though the excess 20% was utilized for approval purposes. The ideal qualities for the hyperparameters, considering the minimization of the leftover mistake, are accounted for in Table 2.

B. KERNEL PERFORMANCE COMPARISON

The study aimed to find the best kernel for the CRHS system by training Linear, Polynomial, and Radial Basis Function (RBF) models with the same dataset, predicting PWM values from 6° to 21°. Despite the Linear kernel initially showing a 93.2% correlation, it dropped to 14.7% with linear regression, while the RBF kernel demonstrated the highest correlation factors (98.2% and 99.99% for SVR and interpolation, respectively), leading to its selection for further research.

C. SVR-RBF MODEL K-FOLD VALIDATION

A k-fold validation (k=3) assessed overfitting within the experimental training dataset, with subsets randomly split into 80%-20% training-validation roles. Table 3 presents high and consistent training scores for both sets, along with correlation factors (R2) for validation cases. Fig. 7 illustrates strong clustering of observed and predicted PWM data along the bisector line, indicating the absence of biases and overfitting in the trained

SVR-RBF model. Despite slightly higher deviations for 9° and 12° lean angles ($\sim 7\%$ and $\sim 5\%$ respectively), attributed to a wider range of possible PWM responses, the model demonstrates reliability in predicting values for CRHS system balancing. An average deviation across the $k=3$ folds stands at 1.68% , reaffirming the model's reliability in predicting PWM values and maintaining equilibrium for two-wheeled vehicles, as considered in this research.

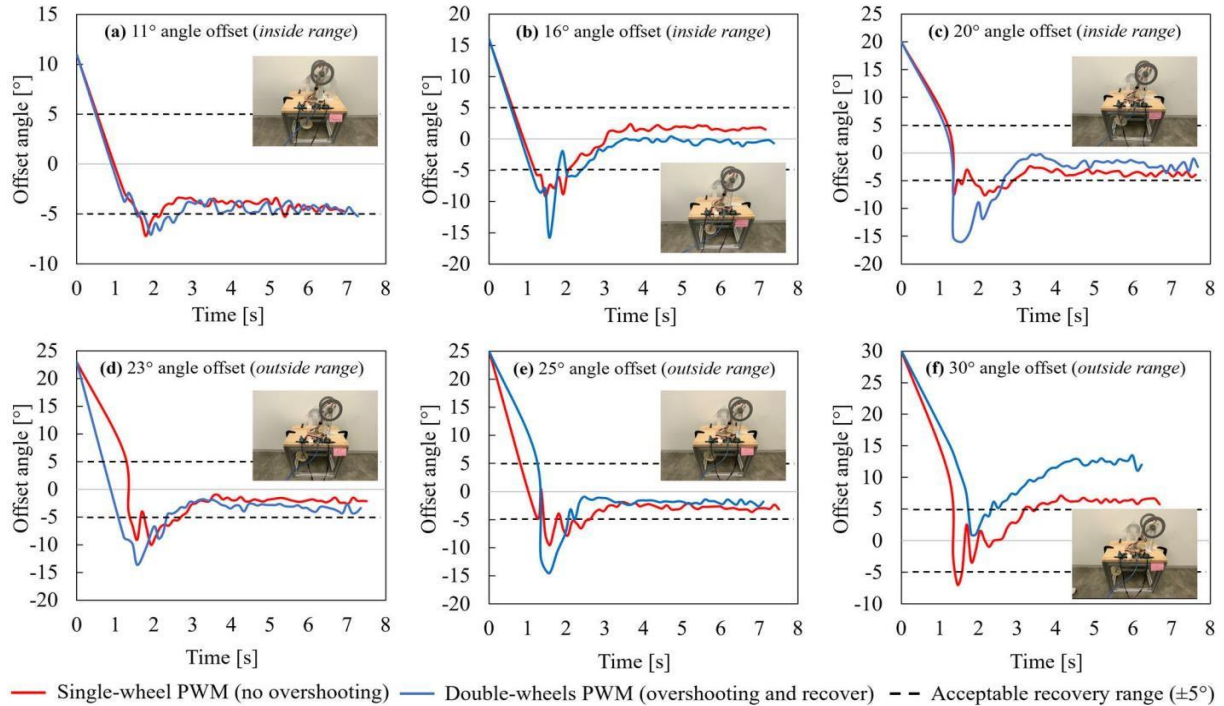


Figure 5: Time-dependent angular recovery within the experimental training range for (a) 11° , (b) 16° , and (c) 20° and outside the training range for (d) 23° , (e) 25° , and (f) 30° initial offset angles.

D. FIELD PERFORMANCES EVALUATION

Experiments were conducted to evaluate the CRHS system's performance, considering the design detailed in Fig. 1 and the experimental procedure outlined in section II-D. Three angles— 11° , 16° , and 20° —not included in the initial SVR model training were examined, with results depicted in Fig. 8a, 8b, and 8c. Red curves, denoted as 'single-wheel PWM', and blue curves, named 'double-wheels PWM', represent correction strategies involving adjustments in one or both wheels, respectively. Successful corrections stabilized the pendulum within a $\pm 5^\circ$ range after applying the initial angular boundary condition, with all scenarios achieving equilibrium in under 2.13 seconds on average. The CRHS system's ability to restore equilibrium within the $\pm 5^\circ$ range, typically in less than 0.47 seconds from the minimum angle, was evident across all experiments except Fig. 8f. Notably, the IMU sensor effectively detected initial overshooting instances, ensuring successful stabilization. Beyond the $\pm 21^\circ$ training range, experiments revealed stabilization challenges for offset angles exceeding 23° , highlighting potential limitations in addressing higher potential energy levels. Further scalability options, such as motor specifications and wheel size adjustments, may be explored to handle inertial forces arising from lean angles beyond 23° .

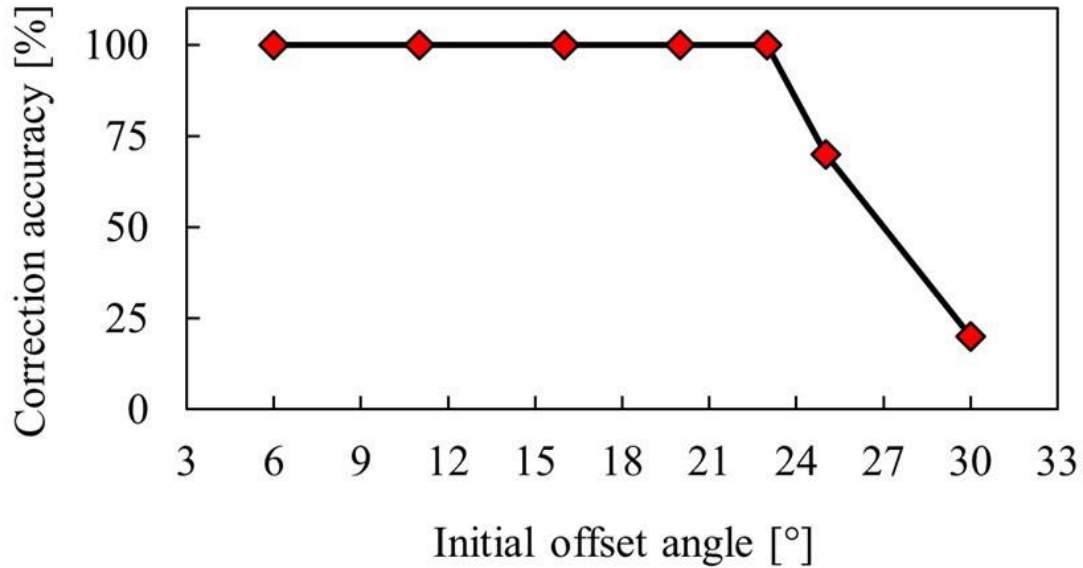


Figure 6: Correction accuracy within and outside the training range of the control SW unit (SVR algorithm).

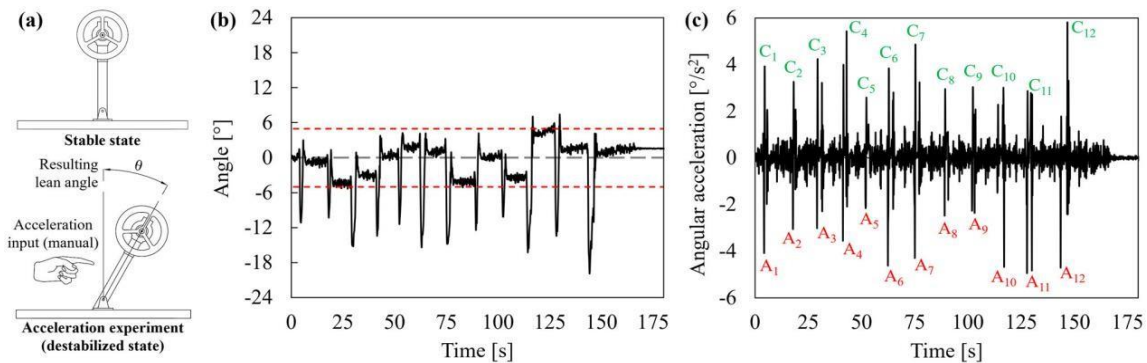


Figure 7. Input (a) and (b) acceleration measured during the random tests utilized to verify the response of the CRHS system under real application conditions.

IV. CONCLUSION

Experiments on a custom-designed lab-scale device validated a two-wheel stabilized design, its hardware (HW), and control software (SW) in this study. In comparison to the results that had been previously published, the Counter-Rotating Hoop Stabilizer (CRHS) system that was proposed showed the following improvements.

- When an offset angle in the "21" range is applied, the control unit, which was based on a Support Vector Regression model and a Radial Basis Function kernel, performed very well in predicting the Pulse Width Modulation (PWM) inputs required by the two independent DC motors to reestablish equilibrium.
- The correction accuracy decreases to 70% (25) and 20% (30) when the offset angle is increased beyond 23 degrees because the specifications of the two DC motors no longer meet the inertia.
- This issue can without much of a stretch be settled by increasing, or even down, the size of the wheels or by utilizing more powerful DC engines to improve the connection capacities of the entire gadget.
- At the point when arbitrary speed increases in the $\pm 6^\circ/s^2$ range were applied to the CRHS framework, adjustment was consistently accomplished inside a normal response season of 1.28s.

A further correction could be successfully carried out by simultaneously correcting the rotational speed (PWM input) for both DC motors in the event that a potential overshooting condition was discovered. From a worldwide point of view, the proposed CRHS plan and controls are general and relevant to different two-wheels vehicles by a legitimate change of the important determinations as per the thought about case.

REFERENCES

- [1]. A. M. El-Nagar, M. El-Bardini, and N. M. El-Rabaie, "Intelligent control for nonlinear inverted pendulum based on interval type-2 fuzzy PD controller," *Alexandria Eng. J.*, vol. 53, no. 1, pp. 23–32, 2014, 10.1016/j.aej.2013.11.006.
- [2]. M. I. Ullah, S. A. Ajwad, M. Irfan, and J. Iqbal, "Non-linear control law for articulated serial manipulators: Simulation augmented with hardware implementation," *Elektronika Elektrotechnika*, vol. 22, no. 1, pp. 3–7, Feb. 10.5755/j01.eee.22.1.14094.
- [3]. M.W. Spong, P. Corke, and R. Lozano, "Nonlinear control of the reaction wheel pendulum," *Automatica*, vol. 37, no. 11, pp.

- 1845–1851, 2001, doi: 10.1016/S0005-1098(01)00145-5.
- [4]. S. G. Khan and J. Jalani, “Realisation of model reference compliance control of a humanoid robot arm via integral sliding mode control,” *Mech. Sci.*, vol. 7, no. 1, pp. 1–8, Jan. 2016, doi: 10.5194/ms-7-1-2016.
- [5]. O. D. Montoya and W. Gil-González, “Nonlinear analysis and control of a reaction wheel pendulum: Lyapunov-based approach,” *Eng. Sci. Technol., Int. J.*, vol. 23, no. 1, pp. 21–29, Feb. 2020, doi: 10.1016/j.jestch.2019.03.004.
- [6]. B. Bapiraju, K. N. Srinivas, P. Kumar, and L. Behera, “On balancing control strategies for a reaction wheel pendulum,” in *Proc. 1st India Annu. Conf. (IEEE INDICON)*, Dec. 2004, pp. 199–204, doi: 10.1109/INDICO.2004.1497738.
- [7]. S. Irfan, A. Mehmood, M. T. Razzaq, and J. Iqbal, “Advanced sliding mode control techniques for inverted pendulum: Modelling and simulation,” *Eng. Sci. Technol., Int. J.*, vol. 21, no. 4, pp. 753–759, Aug. 2018, doi:10.1016/j.jestch.2018.06.010.
- [8]. A. M. El-Nagar and M. El-Bardini, “Practical implementation for the interval type-2 fuzzy PID controller using a low cost microcontroller,” *Ain Shams Eng. J.*, vol. 5, no. 2, pp. 475–487, Jun. 2014, doi: 10.1016/j.asej.2013.12.005.